Annales Geophysicae, 23, 2671–2678, 2005
SRef-ID: 1432-0576/ag/2005-23-2671

Annales Geophysicae

IMF B_Y and the seasonal dependences of the electric field in the inner magnetosphere

H. Matsui[1], **J. M. Quinn**[1], **R. B. Torbert**[1], **V. K. Jordanova**[1], **P. A. Puhl-Quinn**[1], **and G. Paschmann**[2]

[1]Space Science Center, University of New Hampshire, Durham, NH 03824, USA
[2]Max-Planck-Institut für extraterrestrische Physik, 85748 Garching, Germany

Received: 15 February 2005 – Revised: 4 August 2005 – Accepted: 17 August 2005 – Published: 14 October 2005

Abstract. It is known that the electric field pattern at high latitudes depends on the polarity of the Y component of the interplanetary magnetic field (IMF B_Y) and season. In this study, we investigate the seasonal and B_Y dependences in the inner magnetosphere using the perigee ($4<L<10$) Cluster data taken from low magnetic latitudes. The data consist of both components of the electric field perpendicular to the magnetic field, obtained by the electron drift instrument (EDI), which is based on a newly developed technique, well suited for measurement of the electric fields in the inner magnetosphere. These data are sorted by the polarities of IMF B_Z and B_Y, and by seasons or hemispheres. It is demonstrated from our statistics that the electric fields in the inner magnetosphere depend on these quantities. The following three points are inferred: 1) The electric fields exhibit some differences statistically between Cluster locations at the Northern and Southern Hemispheres with the same dipole L and magnetic local time (MLT) values and during the same IMF conditions. These differences in the electric fields might result from hemispherical differences in magnetic field geometry and/or those in field-aligned potential difference. 2) The IMF B_Y and seasonal dependence of the dawnside and duskside electric fields at $4<L<10$ is consistent with that seen in the polar convection cell. In addition, it is possible that these dependences are affected by the ionospheric conductivity and the field-aligned current. 3) The nightside electric field in the inner magnetosphere measured by Cluster is often similar to that in the magnetotail lobe. In the future, it will be necessary to incorporate these dependencies on IMF B_Y and season into a realistic model of the inner magnetospheric convection electric field.

Keywords. Magnetospheric physics (Electric fields; Magnetosphere-ionosphere interactions; Solar wind-magnetosphere interactions)

Correspondence to: H. Matsui
(hiroshi.matsui@unh.edu)

1 Introduction

It is known that electric fields in the polar magnetosphere and ionosphere depend on the Y component of the interplanetary magnetic field (IMF B_Y) (e.g. Cowley, 1981; Burch et al., 1985; Reiff and Burch, 1985; Heppner and Maynard, 1987; Weimer, 1995; Vaith et al., 2004), as well as the season or the tilt angle (e.g. de la Beaujardiere et al., 1991; Crooker and Rich, 1993; Weimer, 1995). Such dependencies are often interpreted in terms of the magnitude and location of the convection cell. The variable location of magnetic reconnection between the IMF and the geomagnetic field is one reason for the IMF B_Y and seasonal dependences. In this case, the dependences of the electric fields on these parameters appear oppositely between hemispheres. In other words, the electric field pattern when IMF $B_Y>0$ ($B_Y<0$) in the Northern Hemisphere is the same as that when IMF $B_Y<0$ ($B_Y>0$) in the Southern Hemisphere. Similarly, the pattern for January (July) in the Northern Hemisphere is the same as that for July (January) in the Southern Hemisphere. Noda et al. (2003) investigated the electric field in the magnetotail lobe and found that the direction of convection is dependent on the polarity of the IMF B_Y component. However, such a study has rarely been performed in the inner magnetosphere. One reason is that this region is thought to be too far inside the magnetopause to see the effect of reconnection. The electric field induced by the interaction of the solar wind and the magnetosphere is modified by the effects of magnetosphere-ionosphere coupling, such as ionospheric shielding (Vasyliunas, 1970, 1972). Another reason is that the IMF B_Z component is a more important parameter controlling the electric field in the inner magnetosphere than the IMF B_Y component and season, so that the IMF B_Z component is often chosen for studies (e.g. Baumjohann and Haerendel, 1985; Goldstein et al., 2002). However, one work by Baumjohann et al. (1986) investigated the dependence of the strength of the inner magnetospheric electric field on IMF B_Y polarity by using data from a geosynchronous satellite GEOS-2 located in the Northern Hemisphere and slightly off the equator. The ratio between the duskside and dawnside electric fields was

larger for negative IMF B_Y than for positive IMF B_Y. This dependence of the electric fields was found to be consistent with the expected location of the convection cell in the polar region.

Our previous statistics using data from the electron drift instrument (EDI) on Cluster demonstrated the IMF B_Z dependence of the electric field in the inner magnetosphere at $4<L<10$ (Matsui et al., 2003, 2004). However, the IMF B_Y and seasonal dependences of the electric field have not been investigated in these works. The electric fields in the Northern and Southern Hemispheres were merged into one data set in our previous database, making it hard to see the IMF B_Y and seasonal dependences when these dependences appear opposite between northern and southern ionospheres. Another problem is that these dependences are expected to disappear at the magnetic equator. However, the actual dependences very near the equator have not been studied. Although Baumjohann et al. (1986) have investigated these problems with GEOS-2, their study was limited to geosynchronous orbit and the dayside sector. The polar orbit of Cluster makes it possible to investigate these problems in the inner magnetosphere at $4<L<10$, at all magnetic local times (MLT), and as will be shown, the electric field depends on these parameters. We examine the origin of the IMF B_Y and seasonal dependence by referring to the size and location of the convection cell, as well as the convection in the magnetotail lobe. This type of study is useful to address which parameter does/does not control the dynamics of the inner magnetosphere in terms of the electric field.

It is also known that the seasonal dependence of the electric field at latitudes $<65°$ is influenced by the ionospheric dynamo (e.g. Richmond et al., 1980). The electric fields caused by the ionospheric dynamo are expected to be the same between hemispheres in the same months, which is different from the dependence of the electric field on season at high latitudes, as described above. For example, the electric field caused by the ionospheric dynamo in the summer season in one hemisphere is the same as that in the winter season in the other hemisphere. This is because the ionosphere in one hemisphere is connected to the ionosphere in the other hemisphere with magnetic field lines, which are considered to be equipotentials. The field lines at low latitudes are short in length between both ionospheres compared to those at high latitudes. Nevertheless, the electric field caused by the ionospheric dynamo during the summer-winter season may be different from that during the spring-autumn season. However, it is hard to see such a seasonal effect of the ionospheric dynamo in our study because the spacecraft stay at one specific range of tilt angle, i.e. only one season for given hemisphere, for each MLT, as discussed below. Hereafter, the term seasonal dependence is used to refer to a dependence that is opposite between hemispheres for the same IMF B_Z and opposite B_Y conditions, and is not caused by the ionospheric dynamo but by the magnetic reconnection.

The organization of this paper is as follows. The data set used in this study and the method of the analysis are described in Sect. 2. The statistical results are presented in Sect. 3, where we show electric potential patterns as well as the relationship between the MLT of spacecraft locations and tilt angle. These results are discussed in Sect. 4, where we consider 1) the similarity of potential patterns, between hemispheres, 2) the dawnside and duskside electric fields compared with the convection cell, and 3) the nightside electric field compared with the electric field in the magnetotail lobe. Finally, conclusions are offered in Sect. 5.

2 Data set and method of analysis

We use both components of the electric field perpendicular to the magnetic field measured by EDI on Cluster (Paschmann et al., 1997, 2001), using data from SC 1, 2, and 3. Data from SC 4 are not available from EDI. The time resolution of the original data depends on the availability of the return beams from the electron guns. The maximum resolution of the routinely processed data used in this paper is 1 s. The data interval of the analysis is more than three years between 18 February 2001 and 10 March 2004, so that the full range of MLT is covered. The electric fields mapped to the equator are derived, in addition to in-situ electric fields in our study. We have mapped the electric fields by using a dipole magnetic field for each 5-min interval of the data. We use the dipole magnetic field instead of a model by Tsyganenko and Stern (1996), unlike Matsui et al. (2004), in order to study the asymmetry of the electric fields between hemispheres in more detail. For the purpose of this mapping it is assumed that there is no electric potential drop along the magnetic field lines. The contribution of the gradient B drift of EDI's electron beams with 500 eV or 1 keV to the measured drift, is estimated using this dipole magnetic field and then removed. The relationship between the L value and the magnetic latitude (MLAT) at the in-situ spacecraft location is shown in Fig. 1. The L values shown in the horizontal axis are between 4 and 10, which we chose as the spatial range of the analysis. Perigee is located at $L\sim4$, where the MLAT is $\sim0°$. As the L value becomes larger, |MLAT| increases to $\sim40°-50°$ at $L=10$. The electric field data in both hemispheres, as defined by the dipole magnetic field, are dealt with separately. The data are further organized by solar wind parameters taken from ACE (Smith et al., 1998; McComas et al., 1998). The propagation delay is taken into account and 40-min averages are used. Average electric fields are calculated at the equator and in-situ locations, for each spatial bin with a size of 1 for L value and 1 h for MLT. Finally, we derive electric potential patterns from the equatorial electric fields using a method similar to that of Matsui et al. (2004).

3 Statistical results

In this section, we show statistical results based on the analysis described in the previous section, beginning with electric potential patterns and then proceeding to the relationship

between the MLT of spacecraft locations and tilt angle in perigee passes.

3.1 Electric potential patterns

The electric potential patterns are calculated for all combinations of the following three conditions: 1) IMF $B_Z>0$, <0, and ~0, 2) IMF $B_Y>0$ and <0, 3) Northern and Southern Hemispheres. We thus calculate twelve potential patterns, as shown below. The potentials are shown for $4<L<10$ and all MLT ranges in the corotating frame. The sorting by Northern or Southern Hemisphere refers to those equatorial potential patterns created from data collected either north or south of the magnetic equator.

First, we show potential patterns for IMF $B_Z<0$ in Fig. 2. The top two panels are the patterns created from Northern Hemispheric data for both IMF B_Y polarities. These two potential patterns show the following IMF B_Y dependence at each MLT sector. The dawnside electric field with IMF $B_Y>0$ tends to be larger than that with IMF $B_Y<0$, while the duskside electric field has a similar strength for both IMF B_Y polarities. The dawn-dusk component of the convection at $L=10$ points duskward (dawnward) in the post-midnight (pre-midnight) with IMF $B_Y>0$. The same component points dawnward on the nightside with IMF $B_Y<0$. The convection on the dayside does not have a clear dependence on IMF B_Y.

Next, we discuss potential patterns created from Southern Hemispheric data, for both IMF B_Y polarities, shown in the bottom two panels of Fig. 2. The electric fields have similar strength between both IMF B_Y polarities on the dawnside and duskside MLT. The dawn-dusk component of the convection at $L=10$ points dawnward on the nightside with IMF $B_Y>0$. The same component points duskward (dawnward) in the post-midnight (pre-midnight) with IMF $B_Y<0$. Skewing of the direction of the convection is seen at $L\sim5$ at ~0 MLT ($\sim$23 MLT) for IMF $B_Y>0$ ($B_Y<0$). Such a signature is also reproduced in numerical simulations (e.g. Garner et al., 2004). The electric field tends to be weaker at pre-noon MLT with IMF $B_Y>0$ than that with IMF $B_Y<0$.

The potential patterns for IMF $B_Z>0$ are shown in Fig. 3. The format of this figure is the same as in Fig. 2. The electric fields for IMF $B_Z>0$ are generally smaller than those for IMF $B_Z<0$. Dawn-dusk asymmetry of the strength of the electric fields tends to exist, which mimics the asymmetry of the electric fields for IMF $B_Z<0$. These two points are consistent with Matsui et al. (2004). The dawnside electric field for IMF $B_Y<0$ is smaller than that for IMF $B_Y>0$ in the Southern Hemisphere. This tendency for the dawnside electric field is weaker in the Northern Hemisphere than in the Southern Hemisphere. The duskside electric field has a similar strength between both polarities of IMF B_Y, in both hemispheres. The dawn-dusk component of the convection at $L=10$ points dawnward (duskward) in the post-midnight (pre-midnight) for both polarities of IMF B_Y, in both hemispheres. The electric field on the dayside is variable between each panel.

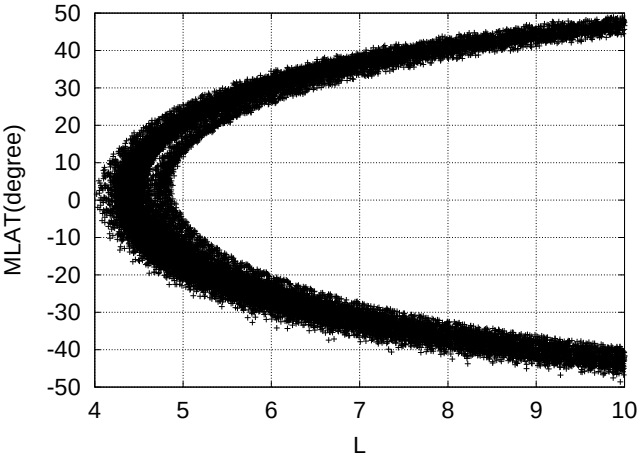

Fig. 1. Relationship between L value and magnetic latitude (MLAT) for our data set. Each data point consists of 5 min average values in our database.

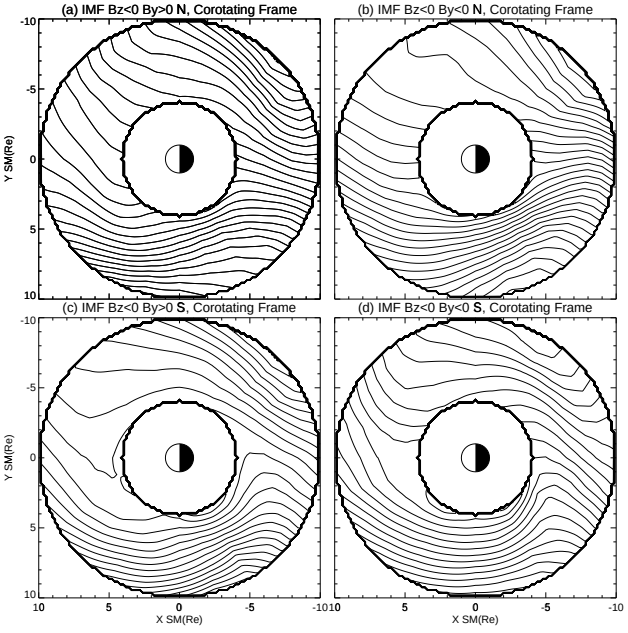

Fig. 2. Electric potential patterns at $4<L<10$ for all MLT ranges. The conditions are IMF $B_Z<0$ and indicated as follows for each panel: **(a)** IMF $B_Y>0$ in the Northern Hemisphere, **(b)** IMF $B_Y<0$ in the Northern Hemisphere, **(c)** IMF $B_Y>0$ in the Southern Hemisphere, **(d)** IMF $B_Y<0$ in the Southern Hemisphere. The patterns are shown in the corotating frame. The contour intervals are 2 kV and 10 kV for thin and thick lines, respectively.

The potential patterns for IMF $B_Z\sim0$ are shown in Fig. 4. The format of this figure is again the same as in Fig. 2. The range of the IMF clock angle is chosen as $75-105°$ ($255-285°$) for the statistics of IMF $B_Y>0$ ($B_Y<0$) with IMF $B_Z\sim0$. These patterns for IMF $B_Z\sim0$ are close to the superposition of the patterns for IMF $B_Z<0$ and $B_Z>0$. The duskside patterns are similar between both IMF B_Y

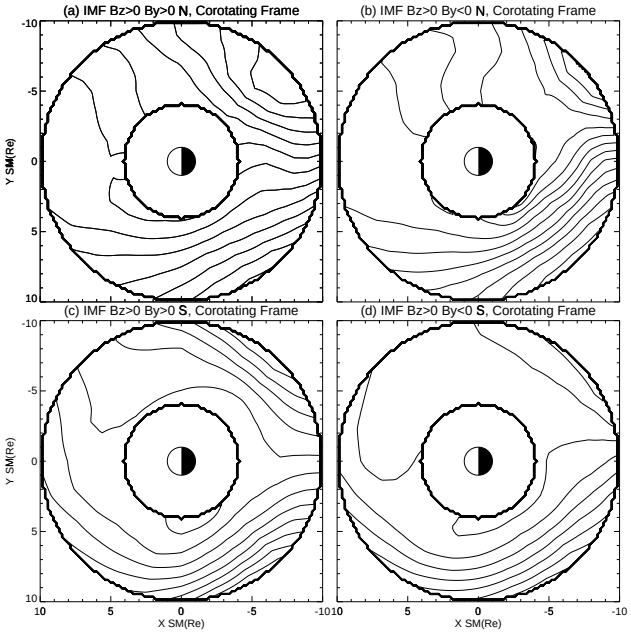

Fig. 3. Electric potential patterns at $4<L<10$ for all MLT ranges. The conditions are IMF $B_Z>0$ and indicated as follows for each panel: **(a)** IMF $B_Y>0$ in the Northern Hemisphere, **(b)** IMF $B_Y<0$ in the Northern Hemisphere. **(c)** IMF $B_Y>0$ in the Southern Hemisphere, **(d)** IMF $B_Y<0$ in the Southern Hemisphere. The patterns are shown in the corotating frame. The contour intervals are 2 kV and 10 kV for thin and thick lines, respectively.

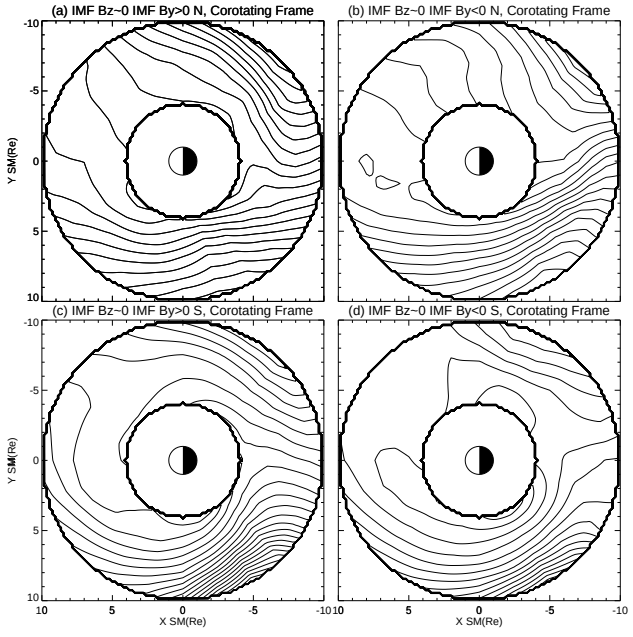

Fig. 4. Electric potential patterns at $4<L<10$ for all MLT ranges. The conditions are IMF $B_Z\sim0$ and indicated as follows for each panel: **(a)** IMF $B_Y>0$ in the Northern Hemisphere, **(b)** IMF $B_Y<0$ in the Northern Hemisphere, **(c)** IMF $B_Y>0$ in the Southern Hemisphere, **(d)** IMF $B_Y<0$ in the Southern Hemisphere. The patterns are shown in the corotating frame. The contour intervals are 2 kV and 10 kV for thin and thick lines, respectively.

polarities. The dawnside electric fields tend to be larger with IMF $B_Y>0$ than with $B_Y<0$. The direction of the nightside electric field is often similar to that with IMF $B_Z<0$. In the following discussion we concentrate on the cases with IMF $B_Z<0$ and $B_Z>0$.

3.2 Relationship between MLT of spacecraft locations and tilt angle

As the perigee of the spacecraft rotates around the Earth once per year, there is a relationship between the MLT of the spacecraft locations and the tilt angle (or season) near perigee, i.e. for $4<L<10$. Figure 5 shows this relationship. The dawnside data are sampled in the winter (summer) season in the Northern (Southern) Hemisphere because the tilt angle takes on negative values. The duskside data are sampled in the summer (winter) season in the Northern (Southern) Hemisphere. The data on the dayside and nightside are obtained around equinox because the tilt angle is close to 0°. It is useful to know these characteristics when we check the seasonal dependence of the electric field in our data set in the following discussion. Another point from this figure is that the seasonal dependence caused by the ionospheric dynamo, which does not have dependence on hemisphere but is different between summer-winter and spring-autumn seasons, is not expected to be seen because observations in one MLT range are fixed to one tilt angle range. If we would like to examine observations in the same MLT range but with another different tilt angle range, it would be necessary to use data from spacecraft with different orbital elements, giving a different relationship between MLT and tilt angle.

4 Discussion

Based on the statistical results described in the above section, we discuss the following three features: 1) similarity of potential patterns between hemispheres, 2) dawnside and duskside electric fields, 3) nightside electric field.

4.1 Similarity of potential patterns between hemispheres

Let us now discuss the similarity of potential patterns between hemispheres as a first step to considering IMF B_Y and seasonal dependences of the electric fields. In Figs. 2 and 3, the equatorial electric potential patterns were created from data that were mapped from either the Northern (top panels) or Southern (bottom panels) hemisphere. In theory, assuming perfect mapping and the absence of parallel electric fields, patterns created from northern data should equal those created from southern data when mapped to the magnetic equator. When we refer to Figs. 2 and 3, the electric fields mapped to the equator are generally similar between Northern and Southern Hemispheres. This is particularly evident for the electric fields on the duskside. However, the electric fields on the dawnside, with IMF $B_Z>0$, and IMF

$B_Y<0$ differ between hemispheres (for example, Figs. 3b and d). We can infer from these points that the electric fields at the in-situ Cluster latitudes are not always similar between hemispheres with the same dipole L and MLT values. One seemingly likely reason for this discrepancy of the electric fields at in-situ locations is that the actual magnetic field has a non-symmetric geometry about the equator and differs from a dipole field. It should be noted, however, that the difference of the electric fields between hemispheres remains even if we substitute the magnetic field modeled by Tsyganenko (2002a, b) for the dipole field. Another possible reason for the discrepancy of the electric fields between hemispheres is different hemispherical field-aligned potential differences along magnetic field lines between Cluster locations and the equator. Note that these two possible sources for the discrepancy of the electric fields, i.e. hemispherical differences in (a) magnetic field geometry or (b) field-aligned potential difference, may coexist.

The potential patterns between both ionospheres are known to be different. It is possible that the electric field at the Cluster location in the Northern Hemisphere is similar to the electric field in the northern ionosphere and vice versa. This point is consistent with the result in Baumjohann et al. (1986), in which the signature of the electric field in one hemisphere of the ionosphere is seen even at the geosynchronous orbit close to the magnetic equator. It should be noted that their observations were made at some 10° to 20° north of the subsolar point, while our observations are made at $0°-50°$ of |MLAT|.

4.2 Dawnside and duskside electric fields

As discussed in Sect. 3.1, there are asymmetries of the electric fields between both IMF B_Y polarities in our statistical result. Although this asymmetry depends on the hemispheres, it is more convenient to discuss data organized by seasons rather than by hemispheres, in order to compare our result with previous ones. It is postulated in the previous paragraph that the electric fields at Cluster latitudes in one hemisphere may be similar to those at the ionospheric level in the same hemisphere. As we have data in both hemispheres, the dawnside and duskside data can be discussed in terms of both summer and winter seasons rather than the original Northern and Southern Hemispheres. In short, we have the following observations: dawnside observations made in winter for the Northern Hemisphere and in summer for the Southern Hemisphere, and duskside observations made in summer for the Northern Hemisphere and in winter for the Southern Hemisphere. The data organized by seasons are used in the following discussion.

Figure 6 shows the ratio of the electric fields for IMF $B_Y>0$ to those for IMF $B_Y<0$. The top and bottom panels are the results for dawnside and duskside, respectively. Each of these two panels contains the ratios for the following four conditions: IMF $B_Z>0$ in summer, IMF $B_Z>0$ in winter, IMF $B_Z<0$ in summer, and IMF $B_Z<0$ in winter. There are three symbols for each condition. A triangle is the ratio at $4<L<10$ estimated from our Cluster data at in-situ locations. The electric fields on the dawnside and duskside are averages in the regions from $3-9$ and $15-21$ MLT, respectively. A square is the ratio at $4<L<10$ estimated from the Weimer model of the ionospheric electric field (Weimer, 2001a), mapped to the Cluster latitudes. A circle is the ratio in the inner magnetosphere expected from the size and location of the convection cell of the Weimer model, as discussed in the next paragraph. Error bars in the figure are calculated by combining averages and standard deviations of the electric

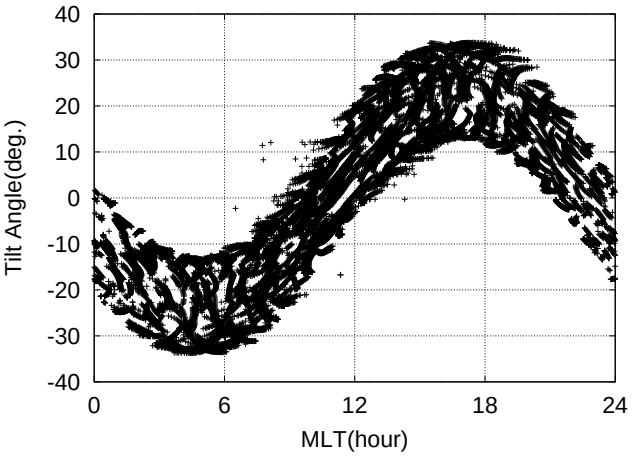

Fig. 5. Relationship between MLT of spacecraft locations and tilt angle in perigee passes. Each data point consists of 5-min average values in our database.

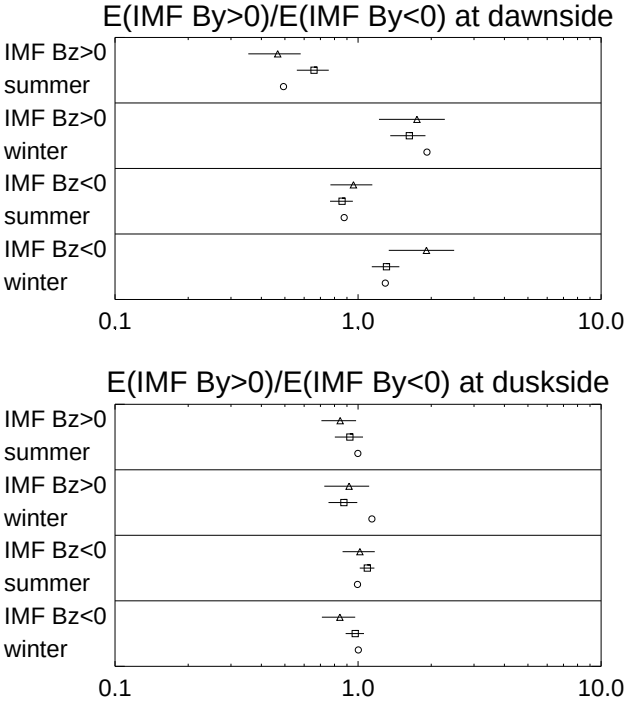

Fig. 6. Ratio of the electric fields for IMF $B_Y>0$ to those for IMF $B_Y<0$ sorted by 1) dawnside and duskside, 2) polarity of IMF B_Z, and 3) summer and winter. See text for the detail.

fields with a bin size of 1 R_E for L and 1 h for MLT. As expected from the potential patterns shown in Figs. 2 and 3, the ratios from Cluster often deviate from 1 on the dawnside. The ratio for IMF $B_Z>0$ in the summer is smaller than 1, while the ratio for both polarities of IMF B_Z in winter is larger than 1. The ratio for IMF $B_Z<0$ in summer is close to 1. The Weimer model at $4<L<10$ predicts a similar ratio as Cluster, although one case for IMF $B_Z>0$ in summer tends to disagree. Although it is not shown in the figure, the ratio can be obtained from GEOS-2 observations made at 9 MLT in the winter season (Baumjohann et al., 1986), yielding a value of 1.8 without discrimination of polarity of IMF B_Z. This value is close to the Cluster values in winter for both polarities of IMF B_Z. It is not possible to compare our result with that from Baumjohann et al. (1986) in summer season because they did not have such measurements. As for the duskside, the ratios are closer to 1 than those on the dawnside for both polarities of IMF B_Z and seasons. This point is common to the result from the Weimer model at $4<L<10$. The ratio from GEOS-2 at 15 MLT is 0.9 (Baumjohann et al., 1986), which is also close to 1.

As noted above, the electric fields in the inner magnetosphere depend on IMF B_Y and season. Such a dependence has often been reported in the polar magnetosphere and ionosphere. If magnetic reconnection at the magnetopause is the reason for this dependence in the inner magnetosphere, as well as in the polar region, we expect the effect of the electric field in the polar region to be similar to that in the inner magnetosphere. We investigate this problem by using the Weimer model. One simplified way to estimate the inner magnetospheric electric field from the polar convection pattern is to calculate |potential(max)|/(MLAT(max)−60) on the dawnside and |potential(min)|/(MLAT(min)−60) on the duskside, where potential(max) and potential(min) are maximum and minimum values of the potential in the Weimer model, respectively. MLAT(max) and MLAT(min) are MLAT of the maximum and minimum values of the potential, respectively. These potential and MLAT values represent the size and location of the convection cell, respectively. The potential size depends on the size of the merged interplanetary electric field, although the offset level is regulated by ionospheric conditions. The dawn-dusk asymmetry of the electric field, which results in the offset level of the potential, is caused by the dayside to nightside asymmetry of the ionospheric conductivity, as suggested by Wolf (1970). The location of the convection cell depends on where the merging process occurs. Furthermore, we assume that the convection cell affects electric fields within a region between MLAT(max) and MLAT of 60°, or between MLAT(min) and MLAT of 60°. Even if we modify this lower boundary of MLAT of 60°, to 50° or 55°, the following discussion is the same. As noted, maximum and minimum values are considered as the observations on the dawnside and duskside, respectively. Most of the potential(max) or potential(min) found in this study are located in the expected MLT sector, dawnside or duskside, except for one, the potential(max) in winter with IMF $B_Z>0$ and $B_Y<0$.

We next calculate the ratios of |potential|/(MLAT−60) with IMF $B_Y>0$ to that with IMF $B_Y<0$, in order to compare them with those obtained at $4<L<10$ from the Cluster data. The results calculated are indicated by circles in Fig. 6. When Cluster ratios indicated by triangles show a deviation from 1, it tends to also be true for the Weimer model ratios, estimated from the size and location of the convection cell indicated by circles. When Cluster ratios are close to 1, the same holds for the Weimer model ratios. Therefore, it is possible the the electric fields in the polar region are related to those in the inner magnetosphere. The potential pattern in the polar region in the summer season is known to be different from that in the winter season because the lobe convection cell might appear as a summer phenomenon (Crooker and Rich, 1993). This may explain the discrepancy between summer and winter electric fields at $4<L<10$, as measured by Cluster.

An alternative explanation for the IMF B_Y and seasonal dependence of the electric fields is found in the influences of ionospheric conductivity and field-aligned currents on the electric fields. Ionospheric conductivity is largely affected by solar illumination, which is dependent on season, as well as precipitating electrons (e.g. Blomberg and Marklund, 1988). Precipitating electrons are one of the carriers of the upward field-aligned current, which is affected by IMF B_Y and season (e.g. Weimer, 2001b). The field-aligned current flowing in our spatial bins might correspond to the upward and downward region 2 currents on the dawnside and duskside, respectively. The ionospheric conductivity on the dawnside tends to be modified compared to that on the duskside because of precipitating electrons carrying upward field-aligned current, which might be one reason for the deviation of the ratio from 1 on the dawnside. Quantitative comparison between the electric field, field-aligned current, and conductivity for each categorization of IMF orientation and season is left as a future work. Finally, it should be noted that the possibility suggested in this paragraph is not independent of the possibility suggested in the previous paragraphs, because the offset of the potentials of the convection cell depends on ionospheric conditions. The electric field in the inner magnetosphere is related to that in the polar region, as well as the conditions in the ionosphere connected to the inner magnetosphere with the same magnetic field lines.

4.3 Nightside electric field

We now discuss the nightside observations. As mentioned in Sect. 3.1, the dawn-dusk component of the convection at $L=10$ with IMF $B_Z<0$ points duskward (dawnward) in the post-midnight (pre-midnight) for IMF $B_Y>0$ in the Northern Hemisphere, while the same component points dawnward for IMF $B_Y<0$. This dawn-dusk component of the convection at $L=10$ with IMF $B_Z<0$ points dawnward for IMF $B_Y>0$ in the Southern Hemisphere, while the same component points duskward (dawnward) in the post-midnight (pre-midnight) for IMF $B_Y<0$. It should be noted that seasonal differences between hemispheres for nightside MLT values might not be

seen in the Cluster data set because the observations are made around equinox. It is expected that only the IMF B_Y effect is seen between hemispheres. Noda et al. (2003) has reported the dependence of the electric field in the magnetotail lobe on IMF B_Y as well as on hemisphere by using the data from Cluster EDI. The direction of the dawn-dusk component of the convection tends to be consistent with the expected location of the reconnection as follows: duskward for IMF $B_Y>0$ and dawnward for IMF $B_Y<0$ in the Northern Hemisphere; dawnward for IMF $B_Y>0$ and duskward for IMF $B_Y<0$ in the Southern Hemisphere. Our results are consistent with Noda et al. (2003), except for the duskside for IMF $B_Y>0$ in the Northern Hemisphere and for IMF $B_Y<0$ in the Southern Hemisphere. One possible reason for this small inconsistency is the skewing of the streamlines of the convection outside the statistical bins between the magnetotail lobe and the inner magnetosphere. According to Hori et al. (2000), the direction of the magnetotail convection is variable at a distance from Earth between -30 and $-10\ R_E$ in the plasma sheet. It should also be noted that there are fewer data points for statistics and/or gaps in the EDI data on the nightside (Matsui et al., 2004). In the future, we plan to add data from probe and particle measurements on Cluster, in order to supplement the nightside data.

5 Conclusions

We have analyzed two perpendicular components of the electric field from Cluster EDI, which is based on a newly developed technique well suited for measurements of the electric fields in the inner magnetosphere. The electric fields are obtained around perigee from $4<L<10$ and at all MLT ranges for a data interval of more than three years. Electric potential patterns were calculated by solving an inverse problem for both IMF B_Y polarities and for both hemispheres, and the data were further organized by IMF $B_Z<0$, $B_Z>0$, and $B_Z\sim0$. Our statistical analysis shows that the electric fields in the inner magnetosphere are indeed dependent on the polarity of IMF B_Y, and on season or hemisphere. Studies related to this topic are rare in the past, which is different from studies on the polar region. For each categorization of IMF B_Z, the strength of the electric field on the dawnside depends on IMF B_Y and hemispheres. The strength of the electric field on the duskside is similar for each polarity of IMF B_Y and hemisphere. The direction of the nightside electric field at $L=10$ depends on IMF B_Y and hemisphere.

The following three points are inferred from the statistics: (1) The electric fields with the same IMF B_Z and B_Y conditions exhibit some differences statistically between spacecraft locations between hemispheres. Two possible reasons for these different electric fields are hemispherical differences in magnetic field geometry at $4<L<10$, and those in the field-aligned potential difference, which are often neglected in simulations and data analyses. (2) When we organize the data by season instead of hemisphere, it is possible to compare our results with those from previous ones and to interpret our data. Our results are consistent with Baumjohann et al. (1986) and Weimer (2001a). We found that the IMF B_Y and seasonal dependence of the dawnside and duskside electric fields in the inner magnetosphere is likely to be related to that in the polar region, because the ratios of the electric fields between both IMF B_Y polarities are similar between the Cluster results and the results estimated from the size and location of the polar convection cell of the Weimer model. Another reason for this dependence might be the influences of ionospheric conductivity and of field-aligned current on the electric fields. (3) The convection on the nightside is often consistent with that in the magnetotail lobe, although this is not always true, presumably because of the skewing of the electric fields between the magnetotail lobe and the inner magnetosphere. These results imply that it is necessary to incorporate these IMF B_Y and seasonal dependences into any realistic convection electric field model in the inner magnetosphere. This requires more data from spacecraft with different orbital elements than Cluster, in order to independently establish MLT and seasonal dependences.

Acknowledgements. We thank the many members of the EDI team for innumerable contributions to the design, development, and operation of EDI and to the ground processing of the data. Discussion with R. Nakamura is helpful for our study. We are grateful to A. Balogh and the Cluster FGM team for providing the magnetic field data used by EDI onboard and in ground processing and to N. Cornilleau-Wehrlin and the STAFF team for providing the onboard STAFF data. We thank N. F. Ness and D. J. McComas for the ACE MAG and SWEPAM data provided through CDA website, respectively. This work was supported by NASA through grants NAG5-9960, NNG04GA46G, and NAG5-13512.

Topical Editor T. Pulkkinen thanks P. T. Newell and another referee for their help in evaluating this paper.

References

Baumjohann, W. and Haerendel, G.: Magnetospheric convection observed between 06:00 and 21:00 LT: Solar wind and IMF dependence, J. Geophys. Res., 90, 6370–6378, 1985.

Baumjohann, W., Nakamura, R., and Haerendel, G.: Dayside equatorial-plane convection and IMF sector structure, J. Geophys. Res., 91, 4557–4560, 1986.

Blomberg, L. G. and Marklund, G. T.: The influence of conductivities consistent with field-aligned currents on high-latitude convection patterns, J. Geophys. Res., 93, 14 493–14 499, 1988.

Burch, J. L., Reiff, P. H., Menietti, J. D., Heelis, R. A., Hanson, W. B., Shawhan, S. D., Shelley, E. G., Sugiura, M., Weimer, D. R., and Winningham, J. D.: IMF B_y-dependent plasma flow and Birkeland currents in the dayside magnetosphere, 1, Dynamics Explorer observations, J. Geophys. Res., 90, 1577–1593, 1985.

Cowley, S. W. H.: Magnetospheric asymmetries associated with the y-component of the IMF, Planet. Space Sci., 29, 79–96, 1981.

Crooker, N. U. and Rich, F. J.: Lobe cell convection as a summer phenomenon, J. Geophys. Res., 98, 13 403–13 408, 1993.

de la Beaujardiere, O., Alcayde, D., Fontanari, J., and Leger, C.: Seasonal dependence of high-latitude electric fields, J. Geophys. Res., 96, 5723–5735, 1991.

Garner, T. W., Wolf, R. A., Spiro, R. W., Burke, W. J., Fejer, B. G., Sazykin, S., Roeder, J. L., and Hairston, M. R.: Magnetospheric

electric fields and plasma sheet injection to low L-shells during the 4–5 June 1991 magnetic storm: Comparison between the Rice Convection Model and observations, J. Geophys. Res., 109(A02214), doi:10.1029/2003JA010208, 2004.

Goldstein, J., Spiro, R. W., Reiff, P. H., Wolf, R. A., Sandel, B. R., Freeman, J. W., and Lambour, R. L.: IMF-driven overshielding electric field and the origin of the plasmaspheric shoulder of May 24, 2000, Geophys. Res. Lett., 29(16), 1819, doi:10.1029/2001GL014534, 2002.

Heppner, J. P. and Maynard, N. C.: Empirical high-latitude electric field models, J. Geophys. Res., 92, 4467–4489, 1987.

Hori, T., Maezawa, K., Saito, Y., and Mukai, T.: Average profile of ion flow and convection electric field in the near-earth plasma sheet, Geophys. Res. Lett., 27, 1623–1626, 2000.

Matsui, H., Quinn, J. M., Torbert, R. B., Jordanova, V. K., Baumjohann, W., Puhl-Quinn, P. A., and Paschmann, G.: Electric field measurements in the inner magnetosphere by Cluster EDI, J. Geophys. Res., 108(A9), 1352, doi:10.1029/2003JA009913, 2003.

Matsui, H., Jordanova, V. K., Quinn, J. M., Torbert, R. B., and Paschmann, G.: Derivation of electric potential patterns in the inner magnetosphere from Cluster EDI data: Initial results, J. Geophys. Res., 109(A10202), doi:10.1029/2003JA010319, 2004.

McComas, D. J., Bame, S. J., Baker, P., Feldman, W. C., Phillips, J. L., Riley, P., and Griffee, J. W.: Solar wind electron proton alpha monitor (SWEPAM) for the advanced composition explorer, Space Sci. Rev., 86, 563–612, 1998.

Noda, H., Baumjohann, W., Nakamura, R., Torkar, K., Paschmann, G., Vaith, H., Puhl-Quinn, P., Förster, M., Torbert, R., and Quinn, J. M.: Tail lobe convection observed by Cluster/EDI, J. Geophys. Res., 108(A7), 1288, doi:10.1029/2002JA009669, 2003.

Paschmann, G., Melzner, F., Frenzel, R., et al.: The Electron Drift Instrument for Cluster, Space Sci. Rev., 79, 233–269, 1997.

Paschmann, G., Quinn, J. M., Paschmann, G. , Quinn, J. M., Torbert, R. B., Vaith, H., McIlwain, C. E., Haerendel, G., Bauer, O. H., Bauer, T., Baumjohann, W., Fillius, W., Förster, M., Frey, S., Georgescu, E., Kerr, S. S., Kletzing, C. A., Matsui, H., Puhl-Quinn, P. and Whipple, E. C.: The Electron Drift Instrument on Cluster: overview of first results, Ann. Geophys., 19, 1273–1288, 2001, **SRef-ID: 1432-0576/ag/2001-19-1273**.

Reiff, P. H. and Burch, J. L.: IMF B_y-dependent plasma flow and Birkeland currents in the dayside magnetosphere, 2, A global model for northward and southward IMF, J. Geophys. Res., 90, 1595–1609, 1985.

Richmond, A. D., Blanc, M., and Emery, B. A., et al.: An empirical model of quiet-day ionospheric electric fields at middle and low latitudes, J. Geophys. Res., 85, 4658–4664, 1980.

Smith, C. W., L'Heureux, J., Ness, N. F., Acuña, M. H., Burlaga, L. F., and Scheifele, J.: The ACE magnetic fields experiment, Space Sci. Rev., 86, 613–632, 1998.

Tsyganenko, N. A.: A model of the near magnetosphere with a dawn-dusk asymmetry 1. Mathematical structure, J. Geophys. Res., 107(A8), 1179, doi:10.1029/2001JA000219, 2002a.

Tsyganenko, N. A.: A model of the near magnetosphere with a dawn-dusk asymmetry 2. Parameterization and fitting to observations, J. Geophys. Res., 107(A8), 1176, doi:10.1029/2001JA000220, 2002b.

Tsyganenko, N. A. and Stern, D. P.: Modeling the global magnetic field of the large-scale Birkeland current systems, J. Geophys. Res., 101, 27 187–27 198, 1996.

Vaith, H., Paschmann, G., and Quinn, J. M., et al.: Plasma convection across the polar cap, plasma mantle and cusp: Cluster EDI observations, Ann. Geophys., 22, 2451–2461, 2004, **SRef-ID: 1432-0576/ag/2004-22-2451**.

Vasyliunas, V. M.: Mathematical models of magnetospheric convection and its coupling to the ionosphere, in Particles and Fields in the Magnetosphere, (Ed.) McCormac, B. M., D. Reidel, Dordrecht, Netherlands, 60–71, 1970.

Vasyliunas, V. M.: The interrelationship of magnetospheric processes, in Earth's Magnetospheric Processes, (Ed.) McCormac, B. M., D. Reidel, Dordrecht, Netherlands, 29–38, 1972.

Weimer, D. R.: Models of high-latitude electric potentials derived with a least error fit of spherical harmonic coefficients, J. Geophys. Res., 100, 19 595–19 607, 1995.

Weimer, D. R.: An improved model of ionospheric electric potentials including substorm perturbations and applications to the Geospace Environment Modeling 24 November 1996, event, J. Geophys. Res., 106, 407–416, 2001a.

Weimer, D. R.: Maps of ionospheric field-aligned currents as a function of the interplanetary magnetic field derived from Dynamics Explorer 2 data, J. Geophys. Res., 106, 12 889–12 902, 2001b.

Wolf, R. A.: Effects of ionospheric conductivity on convective flow of plasma in the magnetosphere, J. Geophys. Res., 75, 4677–4698, 1970.